Journal of Volcanology and Geothermal Research 194 (2010) 15–26

Contents lists available at ScienceDirect

Journal of Volcanology and Geothermal Research

journal homepage: www.elsevier.com/locate/jvolgeores

# The Cerro Aguas Calientes caldera, NW Argentina: An example of a tectonically controlled, polygenetic collapse caldera, and its regional significance

I.A. Petrinovic [a,*], J. Martí [b], G.J. Aguirre-Díaz [c], S. Guzmán [e], A. Geyer [d], N. Salado Paz [e]

[a] CICTERRA—Facultad de Ciencias Exactas, Físicas y Naturales, Universidad Nacional de Córdoba, Av. Vélez Sarsfield 1611—X5016GCA—Córdoba, Argentina
[b] Instituto de Ciencias de la Tierra Jaume Almera, CSIC, Lluis Solé Sabaris s/n, 08028 Barcelona, Spain
[c] Centro de Geociencias, Universidad Nacional Autónoma de México, Campus Juriquilla, Querétaro, Qro., 76230, Mexico
[d] CIMNE International Center for Numerical Methods in Engineering, UPC Campus Nord, Edifici C1, Gran Capità, 08034 Barcelona, Spain
[e] IBIGEO—Universidad Nacional de Salta, Mendoza Nº2, CP 4400, Salta, Argentina

ARTICLE INFO

*Article history:*
Received 29 October 2009
Accepted 21 April 2010
Available online 29 April 2010

*Keywords:*
collapse caldera
Central Andes
Puna
ignimbrites
transpression

ABSTRACT

Polygenetic, silicic collapse calderas are common in the central Andes. Here we describe in detail the Cerro Aguas Calientes caldera in NW Argentina, which comprises two caldera-forming episodes that occurred at 17.15 Ma and 10.3 Ma. We analyse the significance of its structural setting, composition, size and the subsidence style of both caldera episodes. We find that the caldera eruptions had a tectonic trigger. In both cases, an homogeneous dacitic crystal-rich (>60 vol.% of crystals) reservoir of batholithic size became unstable due to the effect of increasing regional transpression, which favoured local dilation through minor strike–slip faults from which ring faults nucleated and permitted caldera collapse.

Both calderas are similar in shape, location and products. The 17.15 Ma caldera has an elliptical shape (17 × 14 km) elongated in a N30° trend; both intracaldera and extracaldera ignimbrites covered an area of around 620 km$^2$ with a minimum volume estimate of 140 km$^3$ (DRE). The 10.3 Ma episode generated another elliptical caldera (19 × 14 km), with the same orientation as the previous one, from which intracaldera and outflow ignimbrites covered a total area of about 1700 km$^2$, representing a minimum eruption volume of 350 km$^3$(DRE).

In this paper we discuss the significance of the Cerro Aguas Calientes caldera in comparison with other well known examples from the central Andes in terms of tectonic setting, eruption mechanisms, and volumes of related ignimbrites. We suggest that our kinematic model is a common volcano-tectonic scenario during the Cenozoic in the Puna and Altiplano, which may be applied to explain the origin of other large calderas in the same region.



## 1. Introduction

Silicic collapse calderas constitute a major target in economic geology due to their association with epithermal deposits (Guillou-Frottier et al. 2000; Vigneresse, 2007; Aguirre-Díaz et al. 2008), geothermal reservoirs (Martínez Reyes et al., 2008; López-Hernández et al., 2009), and more recently, with major hydrocarbon reservoirs (Suárez and Márquez, 2007). Silicic calderas are also the source of major ignimbrite eruptions and represent one of the main hazards associated with volcanic activity. The tectonic setting that favours the formation of large silicic calderas is still not well understood. Therefore, additional combined remote sensing and detailed field studies are required to determine the regional and local structural constraints of large silicic calderas.

In the Central Andes ignimbrite province (NW Argentina, N Chile and S Bolivia), 20 collapse calderas have been identified (Fig. 1) but many of the Neogene ignimbrites still have not been correlated to these known emission centres. Many of these calderas have been identified using satellite images such as the Cerro Galán caldera (Francis et al., 1983), but others have required detailed geological mapping of ignimbrite facies and caldera structures to delineate their geometry and reconstruct their history, such as Luingo caldera (Guzmán and Petrinovic, 2008) and Vilama caldera (Soler et al., 2007). Available information reveals that most of the Andean calderas are recurrent in time, showing a polygenetic nature, but there is not a common pattern followed by these calderas. However, a rapid view of satellite images reveals that most of the Andean calderas are associated with major fault zones with orogen-parallel and oblique trends (Riller et al., 2001), but the role of regional and local tectonics on the formation of these calderas still remains speculative.

In this work we study the particular example of the Cerro Aguas Calientes caldera, located in the NW sector of the Argentinean Puna. Two caldera episodes at *ca.* 17 and 10 Ma, respectively, generated

* Corresponding author. CICTERRA—Av. Velez Sarfield 1611, CP X5016GCA—Córdoba, Argentina. Tel.: +54 351 4344983; fax: +54 351 4333199.
*E-mail address:* ipetrinovic@yahoo.com (I.A. Petrinovic).

0377-0273/$ – see front matter © 2010 Elsevier B.V. All rights reserved.
doi:10.1016/j.jvolgeores.2010.04.012

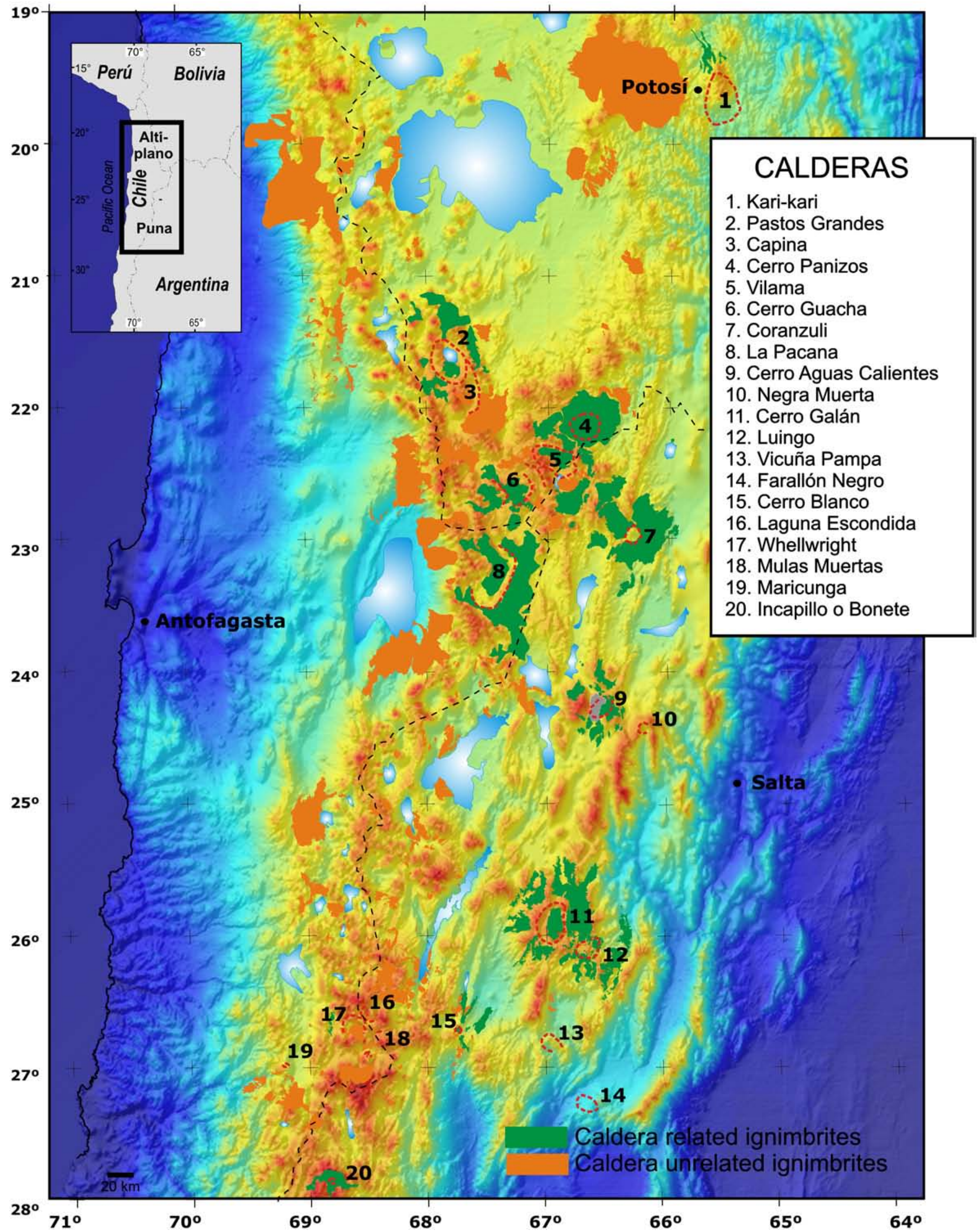


**Fig. 1.** Regional map of the Puna–Altiplano Cenozoic calderas and the present state of knowledge about both caldera-related and unrelated ignimbrites. Caldera names modified from Riller et al. (2001).

similar ignimbrites and caldera depressions in an analogous structural framework. We revise the previous stratigraphy of the Cerro Aguas Calientes caldera proposed by Coira and Paris (1981) and latter modified by Petrinovic (1999). New distribution and volume estimates of the associated ignimbrites are provided, as well as a reinterpretation of the caldera episodes and the structural limits of the resulting depressions. We also analyse the role of the local and regional tectonics on the evolution of caldera-forming episodes. Results are compared with theoretical stages of caldera formation and resurgence (e.g. Marti et al., 1994; Acocella et al., 2004; Holohan et al., 2005, 2008; Geyer et al., 2006).

Finally, we analyse the results obtained in order to check if the Cerro Aguas Calientes caldera constitutes an example of tectonically controlled collapse caldera comparable to other major Andean calderas. A discussion on areas and volumes of calderas and ignimbrites and their significance in the Puna–Altiplano region is also included.

## 2. Geological background and tectonic setting

The stratigraphic basement of the studied area corresponds to the Late Neoproterozoic to Early Cambrian Puncoviscana Formation

(Turner, 1964) (Fig. 2) and is represented by turbiditic sandstones, affected by low-grade metamorphism. The rest of the Palaeozoic sequence is limited to Ordovician rocks in the area, and comprise a plutonic-volcano-sedimentary marine sequence (Coira, 1973; Viramonte et al., 2007). The Cretaceous to Paleocene basins constitute the westernmost outcrops of the northwestern Argentina Cretaceous rift; the Eocene to Recent sequence represents parts of the Andean foreland basin (Hongn et al., 2007; Carrapa and Decelles, 2008).

The Cerro Aguas Calientes caldera is placed on the Precambrian to Ordovician basement that thrusts on Cretaceous to Recent sediments (Fig. 2). This structural pattern is common in the Puna physiography, where bivergent faults delimit narrow valleys within mountain chains. While Neogene sediments fill the intermountain basins, the topographic highs are always made of basement and older rocks.

The Cerro Aguas Calientes caldera is placed 15 km westward of the eastern border of the Puna. This morphological limit includes a protracted deformation belt that has been active from Ordovician to Present time. The Cretaceous outcrops mark the western limit of the NW Argentina rift. These sediments were then inverted in Eocene time, during the early stages of the Andean orogeny (Hongn et al.,

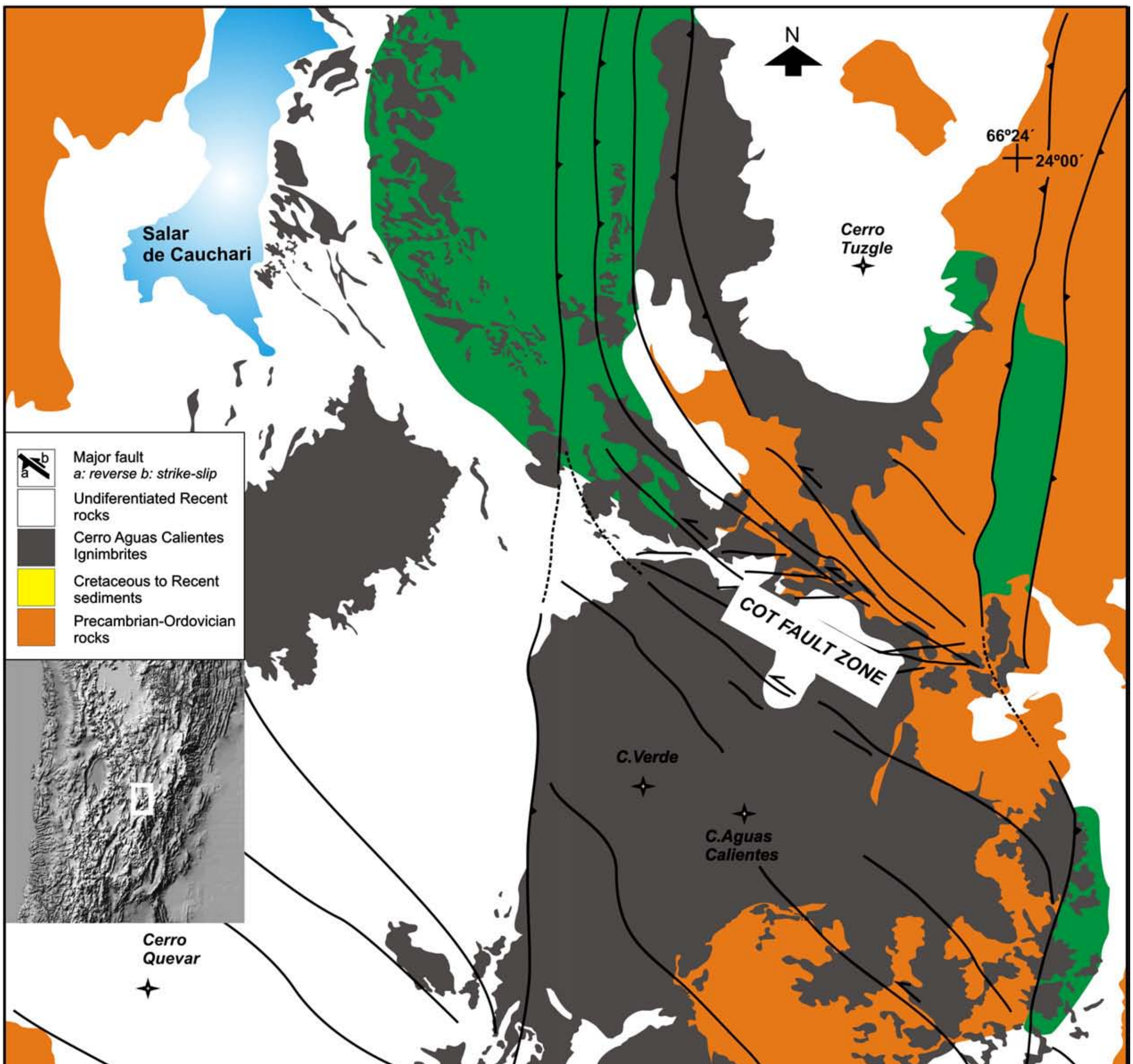


**Fig. 2.** Geological map of the Cerro Aguas Calientes area showing major volcanic units, main structures and basement rocks distribution (modified from Petrinovic et al., 1999).

2007). At present, historic earthquakes >7 in magnitude (e.g. La Poma 1930) evidence neotectonic activity. So, the eastern border of the Puna, from 20°S to 26°S, is a wide, mechanically anisotropic area, which may favour emplacement and ascent of magma, if it is available at depth.

A major fault, the "Calama–Olacapato–El Toro fault zone" (Salfity, 1985; Riller et al., 2001) is delineated by discrete and diverse minor faults, most of which have a left-lateral slip component (Fig. 2). Some volcanic centres are aligned on this major fault, which has traditionally assumed to play a major role in the emplacement of these emission centres (e.g. Matteini et al., 2002; Petrinovic et al., 2005), but also in the formation of some calderas located on the same tectonic lineament (e.g. Negra Muerta Caldera: Riller et al., 2001).

The relationship between these major fault zones and volcanism in the Puna region is a subject of present debate (Viramonte and Petrinovic, 1990; Riller et al., 2001), but only few kinematic studies and tectono-volcanic timing and relations are available (Marret et al., 1994; Riller et al., 2001; Petrinovic et al., 2005, 2006; Mazzuoli et al., 2008).

## 3. Stratigraphy of the Cerro Aguas Calientes caldera

The stratigraphy of the volcanic units of the Cerro Aguas Calientes was formerly proposed by Coira and Paris (1981) and then modified by Petrinovic (1994, 1999). Here, we have unified both stratigraphic frameworks and added new data and interpretations of the area (Figs. 3 and 4).

The volcanic sequence of the Cerro Aguas Calientes caldera includes two major ignimbrites: the Verde and Tajamar ignimbrites.

### 3.1. Verde ignimbrite

This unit, identified by Petrinovic (1994), forms the lowermost unit of the caldera sequence. It is a strongly indurated rock due to welding and devitrification. The base is not exposed and its top is partially covered by the Tajamar ignimbrite. It is a homogeneous pumice-rich deposit, with a characteristic dark to pale green colour and an intense tectonic foliation (Fig. 5A). The pumice fragments are commonly flattened due to welding and show diffuse contacts with the matrix. The Verde ignimbrite is also characterised by the presence of non-vesicular juvenile components (commonly silicified), which have a petrographic and geochemical composition identical to the pumice fragments (Fig. 5B). Crystal fragments are quartz (up to 2 mm), plagioclase (>3 mm), and biotite and hornblende that are generally replaced by hematite–magnetite. Plagioclase crystals commonly show corrosive textures, evidencing disequilibrium growth. The groundmass is vitrophyric, with pyroxene and plagioclase microlites; it is commonly re-crystallised, silicified and mineralised, with Pb–Ag–Zn (Fig. 5C) and Sb–Au veins (Sureda et al., 1986). The crystal content of the pumice fragments (58% vol) is equivalent to that of the matrix and the original glass has been completely devitrified due to vapor-phase and post-emplacement hydrothermal alteration. The latter transformed the original glass into a micro-crystalline aggregate of chlorite, clay minerals, iron–titanium oxides and quartz.

The southern and westernmost outcrops (Figs. 3, 4) exhibit conspicuous breccia lenses, more than 10 m long, composed by granitic and pelitic blocks, up to 60 cm in diameter, from the Ordovician–Precambrian basement and pumice fragments of 0.1 to 8 cm in size, both immersed in an ashy matrix. These breccia lenses are included into the main body of the ignimbrite and are interpreted

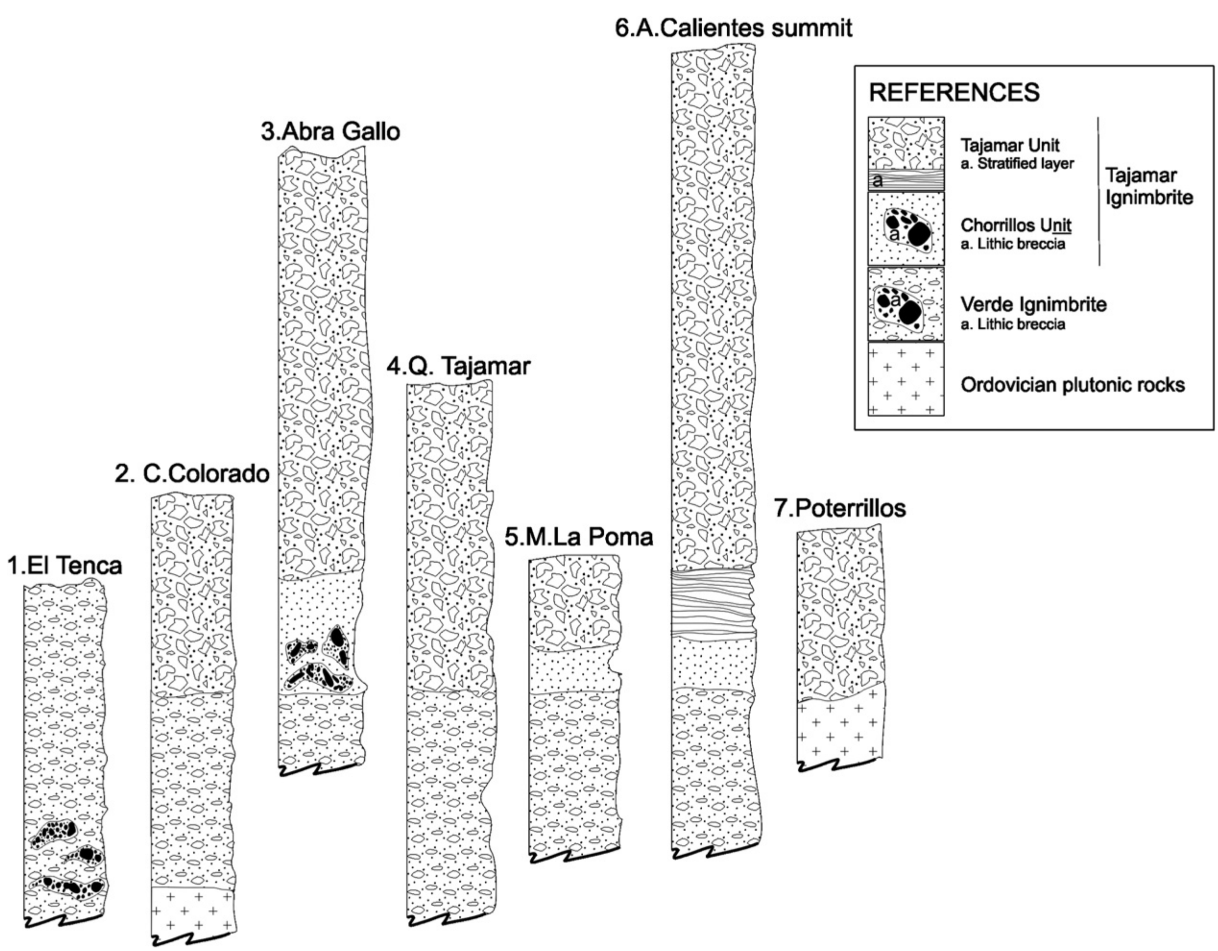


**Fig. 3.** Generalised stratigraphic sections of Aguas Calientes caldera ignimbrites. Location of individual sections is represented by stars in Fig. 4. No vertical and horizontal scales.

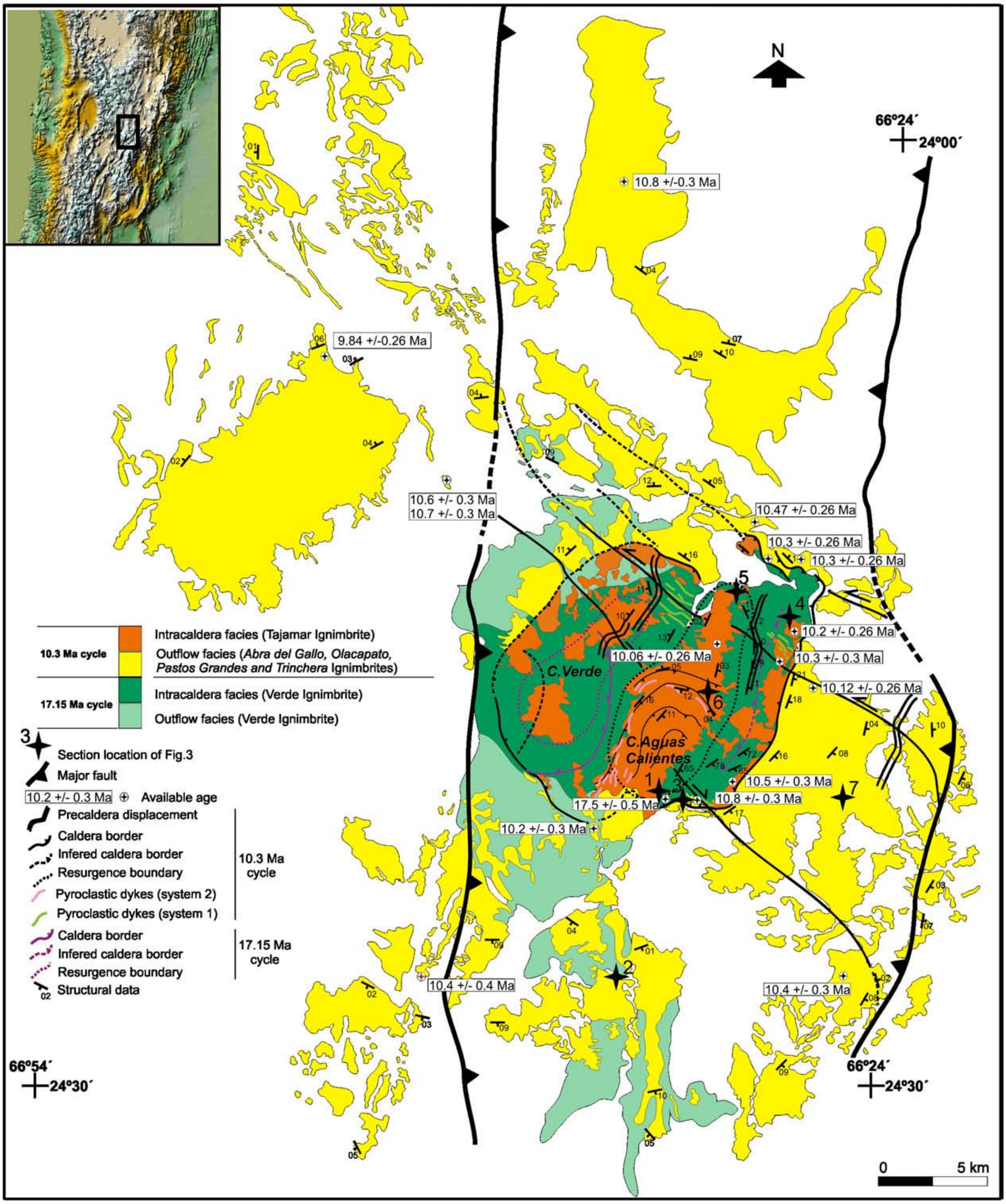


**Fig. 4.** Geological map of the Cerro Aguas Calientes caldera and related ignimbrites (modified from Petrinovic, 1999).

as co-ignimbrite lithic lag breccias, in the sense defined by Druitt and Sparks (1982).

The exposed thickness of the Verde ignimbrite ranges from >520 m at the top of the Cerro Verde (Fig. 4) to 80 m thick in the southernmost outcrops. The area covered by the Verde ignimbrite is of about 650 $km^2$ and the minimum estimated volume is ca. 140 $km^3$ (DRE). In all the volume computations, we have included both primary and extrapolated data. Primary thickness measurements were surveyed at key places in the field (as proximal facies at collar zone, intracaldera sections in the caldera moat, dissected sections at the resurgent domes and distal outflow facies). Intermediate points both in intracaldera and outflow ignimbrites were extrapolated from those and integrated in a grid of thickness data. Volumes were then obtained from solids which were built with commercial software (Surfer + Voxler, Golden software©).

The available K/Ar ages (Petrinovic et al., 1999) for the Verde ignimbrite are shown in Table 1. Also, an age of 17.2 ± 0.5 Ma (K/Ar in biotite) was reported by Olson and Gilzean (1987) Field relationships and field characteristics, such as the presence of a strong tectonic foliation and a marked angular unconformity with the overlying unit, allows the distinction of the Verde ignimbrite (Verde ignimbrite + Aguas Calientes ignimbrite in the sense of Petrinovic et al., 1999) from

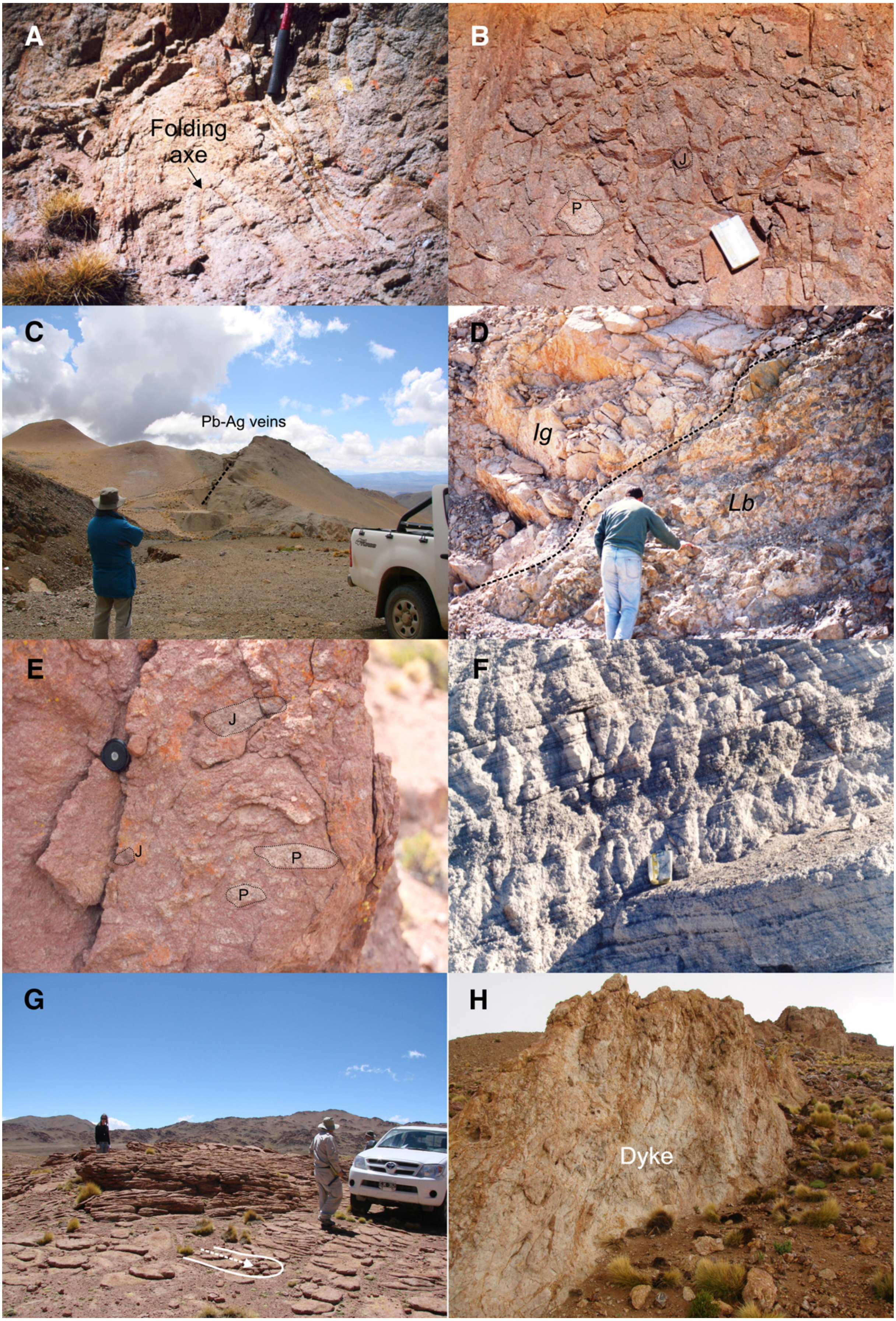
A
Folding
axe
B
J
P
C
Pb-Ag veins
D
Ig
Lb
E
J
J
P
P
F
G
H
Dyke

**Table 1**
Available isotopic ages of the Cerro Aguas Calientes ignimbrites.*

| Sample | Unit | % K | 40 Ar* (nl/g) | 40Ar*/ 40Art | Age (Ma) | 2 σ (Error) |
|---|---|---|---|---|---|---|
| 931242 | Tajamar Ignimbrite (outflow facies) | 7.32 | 2.96 | 0.57 | 10.4 | ±0.3 |
| 931247 | Tajamar Ignimbrite (outflow facies) | 7.03 | 2.85 | 0.64 | 10.4 | ±0.3 |
| 931233 | Tajamar Ignimbrite (outflow facies) | 7.28 | 2.91 | 0.63 | 10.2 | ±0.2 |
| 931234 | Tajamar Ignimbrite (outflow facies) | 7.45 | 3.51 | 0.62 | 12.1 | ±0.4 |
| 891211 | Tajamar Ignimbrite (outflow facies) | 7.3 | 3 | 0.76 | 10.5 | ±0.7 |
| 931212 | Tajamar Ignimbrite (outflow facies) | 7.44 | 3.05 | 0.61 | 10.5 | ±0.2 |
| 89118 | Tajamar Ignimbrite (outflow facies) | 6.75 | 2.59 | 0.72 | 9.8 | ±0.3 |
| 9173 | Tajamar Ignimbrite (Intracaldera–Tajamar unit) | 7.54 | 3.03 | 0.48 | 10.3 | ±0.3 |
| 89114 | Tajamar Ignimbrite (Intracaldera–Tajamar unit) | 7.52 | 3.09 | 0.44 | 10.5 | ±0.3 |
| 941247 | Tajamar Ignimbrite (Intracaldera–Tajamar unit) | 7.04 | 2.94 | 0.85 | 10.7 | ±1.4 |
| 941248 | Tajamar Ignimbrite (Intracaldera–Tajamar unit) | 7 | 2.9 | 0.85 | 10.6 | ±0.3 |
| 9179 | Tajamar Ignimbrite (Intracaldera–Tajamar unit) | 7.47 | 2.93 | 0.78 | 10.1 | ±0.3 |
| 931231 | Tajamar Ignimbrite (Intracaldera–Tajamar unit) | 7.18 | 2.85 | 0.66 | 10.2 | ±0.3 |
| 931223 | Tajamar Ignimbrite (Intracaldera–Tajamar unit) | 6.55 | 2.6 | 0.65 | 10.2 | ±0.3 |
| 931226 | Tajamar Ignimbrite (Intracaldera–Tajamar unit) | 7.24 | 2.86 | 0.69 | 10.1 | ±0.3 |
| 931214 | Tajamar Ignimbrite (Intracaldera–Tajamar unit) | 7.51 | 3.07 | 0.64 | 10.5 | ±0.3 |
| 931229 | Tajamar Ignimbrite (Intracaldera–Chorrillos unit) | 7.64 | 3.11 | 0.38 | 10.4 | ±0.4 |
| 931230 | Tajamar Ignimbrite (Intracaldera–Chorrillos unit-lag breccia) | 7.12 | 3.01 | 0.59 | 10.8 | ±0.3 |
| 891113 | Tajamar Ignimbrite (Intracaldera–Chorrillos unit) | 7.52 | 3.02 | 0.74 | 10.3 | ±0.2 |
| 9178 | Verde Ignimbrite (intracaldera facies) | 7.11 | 2.83 | 0.36 | 10.2 | ±0.3 |
| 931213 | Verde Ignimbrite (intracaldera facies) | 6.15 | 2.4 | 0.65 | 10 | ±0.3 |
| 941206 | Verde Ignimbrite (outflow facies) | 6.99 | 4.41 | 0.83 | 16.2 | ±1.8 |
| 941202 | Verde Ignimbrite (outflow facies) | 7.49 | 5.11 | 0.13 | 17.5 | ±0.5 |
| 941202d | Verde Ignimbrite (lag breccia) | 7.49 | 4.92 | 0.29 | 16.8 | ±0.5 |

*Modified from Petrinovic et al. (1999).
Ar*: radiogenic Argon.
Art: atmospheric Argon.
*K/Ar in pumice biotites.

the younger units (Fig. 3). We validated the 17.5 ± 0.5 Ma date because of its general field relationships and because it is in agreement with the available geochronological determinations (Olson and Gilzean, 1987 and with a recent U/Pb determination of ca. 17 Ma in volcanic clasts from a nearby basin (Petrinovic, unpubl.).

### 3.2. Tajamar ignimbrite

The Tajamar ignimbrite is represented by two units: the Chorrillos and the Tajamar units. Both of them are quite similar in composition and distribution pattern, but were interpreted as two different ignimbrites in previous studies (Petrinovic et al., 1999). However, both units do not show significant differences in their geochronological age determinations (see Table 1). This, together with field evidence such as the absence of erosion or weathered surfaces between the two, suggests that they were erupted in a short time interval, so they can be treated as two units of the same eruptive phase separated by a cooling break and a significant change in the conduit conditions, as we will see below. Therefore, we interpret them to represent a single ignimbrite-forming eruption.

The Chorrillos unit (Chorrillos ignimbrite in Petrinovic et al., 1999) unconformably overlies the Verde ignimbrite. It is a grey coloured, pumice-rich deposit. Pumice fragments are less than 5 cm in diameter, rounded and poorly vesiculated (ca. 35 vol.%), with 40 vol.% of crystal fragments of quartz, sanidine, plagioclase, biotite and magnetite/hematite. The bulk matrix of the deposit has a crystal content proportionally equivalent to that of the pumices. It is a strongly devitrified pumiceous ash, which was transformed into smectite/illite association, and contains lithoclasts of pelites from the basement, up to 7 cm in diameter.

In the southern outcrops, the Chorrillos unit also contains breccia lenses of pumice and basement-derived lithic fragments (granitoids, lavas and pelites 5 to 200 cm in size) supported in an ashy matrix (Fig. 5D). Some lithic clasts of tourmalinic and garnetiferous granitoids, which do not crop out in the region, occur within these breccia lenses. These breccia lenses are interpreted as co-ignimbrite lithic lag breccias, with clasts apparently derived from subsurface units at the vents of this ignimbrite.

At the eastern side the maximum thickness of this unit is 120 m, while at the top of the Cerro Aguas Calientes, the ignimbrite is only 35 m thick (Fig. 3). The ages of the Chorrillos unit obtained by Petrinovic et al. (1999) are shown in Table 1. The Tajamar unit always overlies the Chorrillos and is characterized by a red to pale pink unit with 26 vol.% of crystal-rich (60 vol.%) pumice fragments up to 35 cm in diameter in the proximal facies (Fig. 5E). It is composed of highly re-crystallised ashy matrix, with up to 61 vol.% of phenocrysts of plagioclase, quartz, biotite and augite. In proximal facies, is strongly welded, with flattened pumice fragments, and shows a well developed columnar jointing. As in the case of the Verde ignimbrite, the Tajamar unit, in both proximal and distal facies is characterised by the presence of juvenile non-vesiculated fragments, with a composition similar to the pumices and commonly silicified. The characteristic red colour of the proximal facies is interpreted as due to a vapour-phase alteration that led to the oxidation during devitrification of the matrix and pumice fragments, transforming them into a kaolinite–montmorillonite–illite–calcite mineral assemblage. The red colour becomes somewhat little-oxidised pale pink-grey at the distal facies, showing no flattened pumice fragments.

Near to the top of the Cerro Aguas Calientes, the base of the Tajamar unit shows a 4 to 8 m thick finely stratified and reversely graded sets of 4 cm each (Fig. 5F) which grades transitionally to the main ignimbritic deposit. It is interpreted as a fine dilute pyroclastic density current deposit starting a new episode of a major ignimbritic eruption.

The Tajamar ignimbrite shows a clear distinction between intracaldera and outflow facies, which depends on the caldera border considered. Towards the south, the facies transition occurs in a horizontal distance of 800–1000 m. At the northern border, the facies variation is more clear and occurs in a horizontal distance of 500 m, while at the eastern border, this change is abrupt and occurs in 150 m of horizontal distance (Fig. 3). In the later, the intracaldera ignimbrite increases in thickness more than 300 m when climbing the topographic barrier and quickly thinning to 100 m when the flows

**Fig. 5.** Field photographs of: A) folding and alteration of Verde ignimbrite, B) Verde ignimbrite, (j: juvenile unvesiculated fragment, p: pumice fragment); see text for details, C) Mina La Poma veins and fault plane, D) co-ignimbrite lag breccia deposit next to vents close to eastern ring fault, E) detail of Tajamar ignimbrite in intracaldera facies (j: juvenile unvesiculated fragment and p: pumice fragment), F) ground surge deposit at the base of Tajamar ignimbrite in intracaldera facies, G) ramp structures in outflow facies of Tajamar ignimbrite, a white contour delineates an individual ramp with its interpreted strike, H) pyroclastic dykes of Chorrillos unit.

surpassed the ring fault. Size of crystal-rich juvenile fragments, flattening and welding degree of pumice fragments and the presence of well developed columnar jointing decrease drastically in this transition from intracaldera to extracaldera facies. The ignimbrites thickness also varies considerably. In Cerro Aguas Calientes, at the caldera's interior, this ignimbrite has a maximum thickness of 450 m. By contrast, towards the distal outcrops, the Tajamar ignimbrite thins considerably, up to less than 100 m. The estimated total volume of the intracaldera ignimbrite is ca. 100 $km^3$ (DRE) and was computed with the same methodology explained before.

Some ignimbrite units in the neighbouring areas, previously known as *Ignimbrita Olacapato*, *Ignimbrita Pastos Grandes* and *Ignimbrita Abra del Gallo* (Coira and Paris, 1981; Petrinovic, 1994), are reinterpreted here as equivalent to the Tajamar ignimbrite, according to petrographic, geochemical, stratigraphic, geochronological and field characteristics. These outflow facies (see Fig. 4) show an average thickness of 130 m, moderate welding, sub-rounded pumices fragments of 4 cm in diameter, radial distances of more than 30 km from the caldera and the ability to surpass topographic obstacles higher than 100 m. A characteristic feature of the outflow facies, particularly at distal locations, is the presence of well developed flow lineations and ramp structures (Fig. 5G), similar to those found in lava flows and highly welded rheomorphic pyroclastic rocks (e.g. Soriano et al., 2002). The present area of outflow outcrops is around 1400 $km^2$, and the deposit volume estimate is close to 200 $km^3$ (DRE).

Consequently, the minimum area covered by the Tajamar ignimbrite (both intracaldera and outflow facies) is about 2265 $km^2$ and the total estimated volume is around 350 $km^3$ (DRE). Nineteen available isotopic dates (Petrinovic et al., 1999) of this unit range from 12.1 to 9.8 Ma, but the determinations with less error give an average age of 10.3 Ma (Table 1) in coincidence with other available determinations (JICA, 1993).

## 4. Structural features of the Cerro Aguas Calientes caldera

Major N–S trending faults delimit both W and E sides of the Cerro Aguas Calientes area (Figs. 2, 4). The eastern one, thrusts basement rocks on Cretaceous to Recent sediments and the western one, thrusts Cretaceous rocks on Miocene to Pleistocene sediments (Figs. 2, 4). As most of the N–S regional faults in the Puna and Eastern Cordillera, they have reverse component and both eastern and western vergences. Notably, if there is a strike–slip component, it is always subordinated to the vertical one (Petrinovic et al., 2008).

The "Calama–Olacapato–El Toro" (Salfity, 1985; Riller et al., 2001) regional lineament is represented by a family of NW–SE (N330°) minor strike–slip faults that commonly have a left-lateral component; one of these faults delineates the northern caldera rim (Fig. 4). These N330° minor faults in the Cerro Aguas Calientes area are bounded by two N–S trending thrusts, showing a major left-lateral slip motion with subordinated normal component (Fig. 4). Other group of minor faults recognised in the area have a general trend of N70° (NE–SW) and always have a normal with subordinated strike–slip component (Petrinovic et al., 2006).

Ring-fault planes are commonly covered by the caldera-forming unit, where the intracaldera facies grades into the outflow one (see interpretations below), but predominately exhibit the precaldera sequence (Ordovician granitoids). The segments of ring faults that do not have a clear outline, were extrapolated from the apparent ones and are shown in Fig. 4.

Eruption conduits can be recognised as pyroclastic dykes and are tipically placed in the ring fault surroundings and have two main trends. A set of pyroclastic dykes are controlled by fault planes oblique to the caldera rim (System 1; Fig. 4) and another set of pyroclastic dykes outdraw the caldera ring faults (System 2; Fig. 4). Both systems of conduits and their directions constitute paramount evidences for the caldera timing, as will be discussed below.

As a whole, dykes of System 1 trend N330° and correspond to the Chorrillos unit (Fig. 5H), showing the pumice fragments vertically aligned and drastically flattened parallel to the conduits. Dykes thickness is around 1 to 2 m and the length is highly variable with a minimum of 12 m and a maximum of 200 m, with some shaped as a sigmoid (Fig. 4). Associated with System 1, are hydrothermal dykes constituted by silicified breccias cutting the ignimbrite.

System 2 (Fig. 4), is represented by 8 to 17 m thick arcuate pyroclastic dykes that are formed by the Tajamar unit. Distribution of these conduits outdraws a concentric pattern enclosing an area of 7 km in diameter (Fig. 4). As in System 1, pumice fragments are vertically oriented into the conduits.

The Cerro Verde (Fig. 4) is a structural dome with its major axis oriented N30° in coincidence with the major axis of the caldera (Fig. 4). The Verde ignimbrite was structurally uplifted more than 800 m from the inferred caldera border and formed this intracaldera dome. Internal layering or foliation of the Verde ignimbrite dips 20°–25° in both sides of the Cerro Verde (Fig. 4), thus evidencing a final stage of uplift after the ignimbrite deposition and subsequent cooling (Fig. 6).

In the same way, the Cerro Aguas Calientes was uplifted after the Tajamar ignimbrite eruption (Fig. 6). Field evidence of this includes the isolated outcrops of the ignimbrite dipping outward in both west and east slopes and the vertical displacement of intracaldera outcrops and outflow ones (1000 m).

In order to study the pre- and syn-eruptive deformation in the area and the relationship between tectonics and caldera formation, we have obtained a kinematic data set including 40 measurement sites (Fig. 4) from the pre-10.3-Ma caldera rocks (Ordovician granitoids, pelites and the volcanic rocks of the 17.15 Ma episode), considering both major and minor fault planes. The theoretical interpretation of this data set has been integrated with previous regional structural data and major geological observations to provide a more realistic geological approach than with kinematics alone.

## 5. Caldera-forming episodes

Based on the available geochronological data and new field observations and facies correlations, we have identified two caldera-forming episodes in the area of the Cerro Aguas Calientes. A first collapse caldera event occurred at ca. 17.15 Ma (associated with the Verde ignimbrite eruption) and a second one at ca. 10.3 Ma (Tajamar ignimbrite eruption). These two episodes of caldera volcanism were merged into a single one in previous contributions on the same area (Petrinovic et al., 1999) due to their similarity in bulk characteristics and coincidence of some of the early age determinations.

### *5.1. The 17.15 Ma episode*

The outcrop distribution of this caldera-forming episode, in comparison with the later one, suggests the occurrence of major tectonically induced topographic changes in the area, indicated by successive folding and faulting events recorded by different foliation sets in the Verde ignimbrite and a predominant N–S trend gathering of the outcrops (Figs. 4, 5B).

The distribution of outcrops of the Verde ignimbrite and the location of proximal facies (e.g. lithic breccias interpreted as lag breccias) constitute strong evidence for a caldera collapse episode associated with its eruption. The position and characteristics of the caldera rim were modified by the later caldera-forming episode, but the facies distribution of deposits, the presence of topographic rims clearly associated with some of them, and the thickness variations of the Verde ignimbrite, allow us to infer the original collapse borders shown in Fig. 4, which outline a caldera of major proportions.

The 17 Ma peak in volcanic activity appears to be a regional event in the Puna (Coira et al., 1993; Petrinovic et al., 2006). It represents the

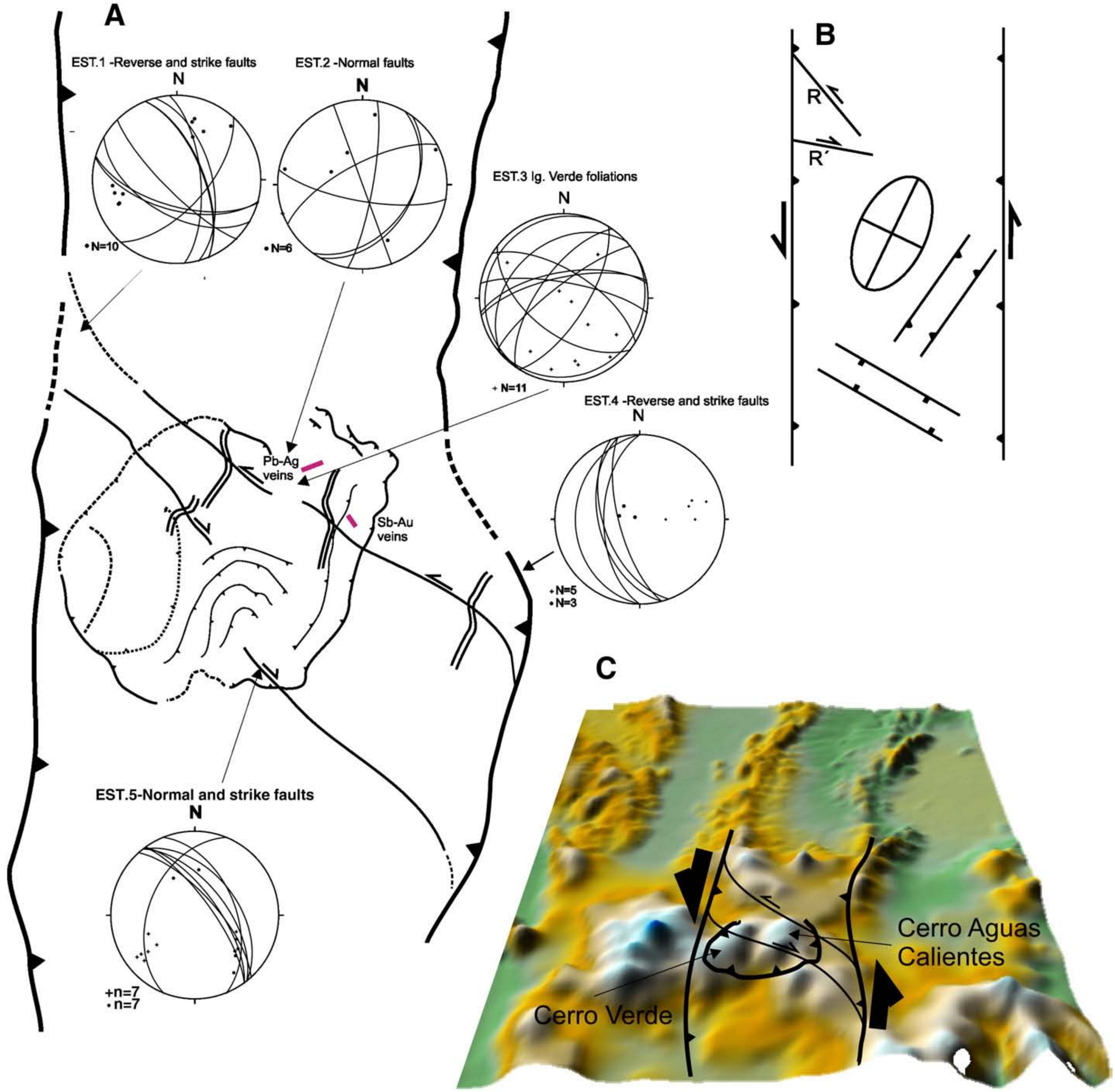


**Fig. 6.** Syn-collapse structural model of the 10.3 Ma cycle in the Cerro Aguas Calientes caldera (theoretical transpressive configuration from Saint Blanquat et al., 1998).

older explosive volcanism recognised in the eastern border of the central and southern Puna.

### 5.2. The 10.3 Ma episode

The 10.3 Ma caldera-forming episode is represented by a thick succession of ignimbrites related to a 220 $km^2$ caldera structure (Fig. 4). Petrinovic et al. (1999) only identified the western border of the caldera, but the new field data allow us to delimit a complete caldera border (19 × 14 km) with the major axis elongated in a N30° trend.

A tumescence episode prior to the caldera collapse is evidenced by changes in dip of ignimbrite outside of the caldera border (see structural data in Fig. 4).

As we described above, two vent systems were identified: System 1 and System 2 (Fig. 4). System 1 is constituted by pyroclastic dykes of the Chorrillos unit with an average strike of N330° (slightly oblique with respect to the main ring fault). System 2 is younger than System 1 and outdraws an arcuate shape enclosing an area of 7 km in diameter (Fig. 4). An abrupt dip change of layers, from vertical to horizontal, next to System 1's pyroclastic dykes (see dip data in Fig. 4), suggests an immediate deposition of the ignimbrite-forming pyroclastic flows around these conduits. The nature of the lithic clasts (Precambrian to Ordovicic basement rocks) of the Chorrillos unit suggests that the fragmentation level was deeper than 500 m (the Verde ignimbrite thickness). The intracaldera pyroclastic flows that formed both Chorrillos and Tajamar units apparently were synchronous with the caldera collapse as they were restricted to the collapsed area in a predominant N–S trend. This suggests that these eruptions were initially controlled by the tectonic structures in the area, and thus, apparently acting as fissural pyroclastic eruptions as described by Aguirre-Díaz and Labarthe-Hernández (2003) for the Sierra Madre Occidental ignimbrites in Mexico. During caldera collapse, new conduits opened in the caldera interior along subvertical and curved fault planes, mostly with reverse component (System 2; Fig. 4). This pattern of conduits propagation agrees with the timing proposed in analogue models (Marti et al., 1994; Acocella et al., 2000). The arcuate pyroclastic dykes favoured the eruption of the Tajamar unit, which does not contain significant proportion of basement-derived lithics, thus indicating a shallower fragmentation level than that for the Chorrillos unit. Crystal-rich (60%) juvenile fragments slightly vesiculated and tipically silicified groundmass were observed.

Moreover, the intracaldera outcrops are irregularly distributed into the caldera and their thickness is not homogeneous showing significant variations from one outcrop to another. This suggests that the original collapsed surface was topographically irregular (Fig. 4), which may be a consequence of the pre-collapse deformation in the area.

The caldera-forming episode ended with a generalised resurgence and a caldera moat around the resurgent structural dome (Figs. 4, 6). The topographic difference between the caldera moat and the eastern border of the caldera suggests a resurgence uplift of approximately 1000 m of the intracaldera block.

Resurgence caused inversion of the subvertical collapse faults of System 2 re-accommodating the blocks in the Cerro Aguas Calientes summit (Fig. 4). During or after resurgence, localised hydrothermal base and precious metal veins occurred at the caldera interior close to ring faults. Two epithermal systems of Pb–Ag–Zn (La Poma mine) and Sb–Au (Incachule mine) were set on tensional fractures (Fig. 4). The latter, was placed in 12 veins with different degrees of mineralisation in the same fault planes than the pyroclastic dykes of System 1 (Fig. 4) in a N330°–N350° trend and lengths of 600 m. The mineral association is antimonite, arsenopyrite and pyrite with quartz (Blasco et al., 1996) probably enriched in depth (JICA, 1993). The other epithermal system (La Poma mine) constitutes a major vein system with N70° in trend, 600 to 1200 m in length and variable thickness between 0.10 and 0.30 m. The mineralisation consists of argentiferous galena, pyrite, calcopyrite and sphalerite associated with tetraedrite, bornite, ullmanite and marcasite with quartz, calcite and siderite (Argañaraz and Sureda, 1979) with scarce supergenic mineralisation. Veins immediately followed the pyroclastic dykes of the 10.3 Ma cycle using the same fault planes. At present, much of the hot springs recognised are placed close to the caldera borders (Incachule, Aguas Calientes, Tocomar and Antuco), some of them noticeable as potential geothermic reserves (Petrinovic and Colombo, 2006).

The characteristics and stratigraphy of the Tajamar ignimbrite, as occurs with the Verde ignimbrite from the previous caldera-forming episode, reveal that Chorrillos and Tajamar units originated during the same caldera-forming event and that both were erupted simultaneously during the subsidence of the caldera block. The lack of plinian deposits preceding the emplacement of the ignimbrites suggests that the onset of the caldera collapse started at the beginning of the eruption, with the emplacement of the co-ignimbrite lag breccias of the Chorrillos unit. It then developed immediately into massive proportions without any previous plinian episode that could decompress the magma chamber. In this sense, the Cerro Aguas Calientes caldera is classified as an overpressure caldera according to Martí et al. (2009). The absence of ash deposits associated with the ignimbrites, the presence of ash in the groundmass, and the similar high content of crystals in the groundmass and pumice fragments suggest that the emplacement of the Cerro Aguas Calientes ignimbrites did not generate significant ash clouds accompanying the main pyroclastic flows. These behaved as massive, dense poorly expanded flows that rapidly transformed into a viscous flow similar to lava flows or rheomorphic tuffs, as it is indicated by the pervasive flow-ramp structures developed in the outflow facies (Fig. 5G).

## 6. The structural control of the calderas and its regional importance

The significant role of regional and local tectonics on the formation of collapse calderas has been documented in several field studies (e.g. Bellier and Sébrier, 1994; Acocella et al., 2002; Spinks et al., 2005; Aguirre-Díaz et al., 2008), as well as in analogue models of collapse calderas developed in tensional and strike–slip environments (e.g. Acocella et al., 2004; Holohan et al., 2005, 2008). In the central Andes, the emplacement of calderas on strike-fault zones has been previously investigated (e.g. Viramonte and Petrinovic, 1990), but up to now, the only example where this relation has been proved and documented is the Negra Muerta caldera (Riller et al., 2001; Ramelow et al., 2005).

There is considerable evidence of the influence of regional and local tectonic structures on the formation of the Cerro Aguas Calientes caldera. As explained in previous sections, it is located on the Calama–Olacapato–El Toro fault zone (Fig. 1), a major strike–slip fault system oriented NW–SE and oblique to the major N–S tectonic trends of the central Andes.

As a result, a left-lateral transpressive setting trending N–S can be interpreted in the Cerro Aguas Calientes area in agreement with theoretical models of left-lateral transpression (Saint Blanquat et al., 1998: Fig. 6) and analogue modelling results (Holohan et al., 2008). A bi-verging and N–S trending fault system with left-lateral component that occurred before or simultaneously to the caldera collapse (Fig. 6) caused local dilation in the N330° straight fault planes and fractures. A shallow reservoir of partially crystallised dacitic magma of batholitic proportions was affected by this tectonic episode and became unstable, facilitating magma chamber rupture and magma fragmentation by a mechanism similar to the one recently proposed by Gottsmann et al. (2009). Magma immediately mobilised and rose to the surface using the N330° system (System 1: Fig. 4), initiating the eruption and subsequent caldera collapse by nucleating the ring fault from the strike–slip system. Caldera subsidence progressed and a new group of collapse faults propagated to a central position of the caldera serving as conduits (Systems 2 in Fig. 4) for the evacuation of major volumes of ignimbrite-forming pyroclastic flows, together with those coming out from the ring faults. As a difference with the linear dykes of the System 1 controlled by tectonic fault planes, these arcuate pyroclastic dykes were purely formed as a consequence of the collapse itself and not along pre-existing tectonic lineations.

The left-lateral transpression active at the time of the caldera formation implies an ENE–WSW shortening direction, which is in agreement with the suggestion of Marret et al. (1994) for the Miocene in the Puna region and coeval with an increase of the crust thickening (Isacks, 1988). For the same area, Petrinovic and Colombo (2006) proposed a NE–SW Quaternary shortening, which is also valid for the Quaternary volcanism of the northern Calchaqui Valley, at the eastern Puna border (Guzmán et al., 2006).

Nevertheless, if the N70° tensional faults controlling Pb–Ag–Zn veins (Fig. 4) are considered as coeval with the N330° ones with pyroclastic dykes and Sb–Au veins, the change of shortening direction in time, must be not applicable. The solution of both tensional directions coeval into the same structural model could be drawn if an orogen-parallel stretching (Riller et al., 2001; Riller and Oncken, 2003) is considered. Hence, the Quaternary shortening direction proposed by Petrinovic and Colombo (2006) reinforces this suggestion. Therefore, a combination of left-lateral transpression with NE–SW shortening direction and NS stretching fulfills the proposed local structural model proposed and accounts for the presence of both tensional systems in the same model.

There is no evidence for the kinematics preceding and controlling the first (17.15 Ma) caldera collapse of the Cerro Aguas Calientes.

However, we infer similar kinematics and caldera collapse conditions for both episodes because of the ring fault position, the caldera and resurgence axes, and the coincident bulk distribution of facies.

This particular case of left-lateral transpression favouring a caldera collapse is probably not unique in the central Andes. Many of the largest Andean calderas, such as La Pacana, Galán and Panizos, could be probably explained with a similar structural model. More interesting would be to look for the same tectonic framework in those calderas that are still poorly known. Considering the model of rhomb-shaped domains proposed by Riller and Oncken (2003), most of the calderas—and generically volcanoes—confined by transpressive ranges in the Central Andes could be originated in the same manner as we proposed here.

In order to adequately quantify the potential number of calderas in this situation, we have calculated the total area, and estimated volume, of the ignimbritic field in the Altiplano-Puna region. The final objective is to calculate approximately how much of this ignimbritic volume is related to known calderas and how much remains unrelated to recognised emission centres. Fig. 1 summarises the present state of knowledge about ignimbrites and calderas in this region. Outcrops of Neogene ignimbrites between 18° and 28°S cover an area of 44,000 $km^2$, which contrasts with the 70,000 $km^2$ proposed by de Silva et al (2006) for the Altiplano–Puna Volcanic Complex (APVC; 21°–24°S). If the surface presumably occupied by ignimbrites but completely eroded out is also considered, then the total area might be increased by 25%, giving a value close to the 55,000 $km^2$. The Puna–Altiplano area between 18°S–28°S and 69°W–66°W is of on the order of 280,000 $km^2$, so the Neogene ignimbritic area is about 20% of the total surface of the Puna–Altiplano area. From the ignimbritic area, only 15,000 $km^2$ (33%) of the total ignimbritic surface is undoubtedly related to the recognised collapse calderas, so 29,000 $km^2$ (66%) of ignimbritic outcrops remain without evident association with known calderas.

Considering a mean thickness of 100 m for the outflow ignimbrites related to calderas, and providing that the intracaldera volume is 2/3 of the total volume erupted in each episode, the volume of the ignimbrites related to calderas is about 4500 $km^3$ and the total volume of ignimbrites related and unrelated to calderas is about 7300 $km^3$. This computation differs again from that of de Silva et al. (2006) by 15,000 $km^3$ for the APVC. Our calculations correspond to the present state of knowledge on the collapse calderas from the Puna–Altiplano and reinforce the need to explain this 66% of “rootless” ignimbrites. Considering that this 33% of caldera-related ignimbrites is associated with 20 major calderas, another 20 collapse-calderas (*sensu lato* Aguirre-Díaz, 2008) could remain unexplored (see e.g. Aguirre-Díaz y Labarthe-Hernández 2003).

## 7. Conclusions

The Cerro Aguas Calientes caldera includes two caldera-forming episodes that occurred at 17.15 Ma and 10.3 Ma respectively. The 17.15 Ma episode is represented by a petrographically homogeneous eruption unit called Verde ignimbrite, with a minimum volume of 140 $km^3$ (DRE) that could increase to 300 $km^3$ if non-exposed outcrops and eroded areas were also estimated. Visible and inferred borders of this caldera encircle an area of 156 $km^2$ with a major axis of 14 km in a N30° trend. Eruption conduits, i.e., ring faults, are outlined by the presence of co-ignimbrite lithic lag breccia deposits along some sectors of the caldera border.

The 10.3 Ma caldera-forming episode is better exposed and we can distinguish the emplacement of two successive cooling units during this episode, the Chorrillos unit, which represents a minimum volume of the eruption and the Tajamar unit, which constitutes the main caldera-forming unit, with a total volume of more than 350 $km^3$ (DRE).

There is strong evidence for a tectonic trigger of the two caldera-forming eruptions. Deformation along the strike–slip fault of the Calama–Olacapato–El Toro, on which the Cerro Aguas Calientes caldera is located, caused pressure disequilibrium in a partially solidified shallow magma chamber of batholithic proportions. These caldera-forming episodes initiated with the tumescence of whole caldera area, probably associated with the growing of the magma chamber. Magma chamber rupture and opening of eruption conduits were favoured by N330° fault planes close to the main ring fault (pyroclastic dykes: System 1) and by the ring fault itself, as it is marked by the presence of co-ignimbrite lithic lag breccias on the southern sector of the caldera border. Progressively, subordinate eruption conduits migrated to the centre of the caldera, forming arcuate and concentric pyroclastic dykes (System 2) that used reverse and subvertical fault planes limiting the collapsing blocks. Geometry and distribution of reverse fault planes are similar to the ones observed in analogue models of collapse calderas, as occurs with the propagation from System 1 at the caldera periphery to the System 2 at the centre of the collapsing zone. As a final stage, 1000 m of resurgence of the caldera moat provoked the present-day configuration with a N30° elongated structural dome at the interior of the caldera.

Structural framework indicates an orogen-parallel transpressive setting, bounded by reverse faults with left-lateral component. This model agrees in part with the ENE–WSW Miocene shortening direction proposed for the Puna.

The structural model proposed to explain the formation of the Cerro Aguas Calientes caldera may be applied to other large calderas in the central Andes that show similar characteristics and are placed in similar local tectonic settings.

The two caldera-forming episodes of the Cerro Aguas Calientes caldera are similar in the eruption sequence and the area and location of the resulting caldera depressions. Both caldera eruptions started and continued with the emission of large volumes of ignimbrite, allowing the caldera collapse to occur from the beginning of the eruption, without any preceding plinian phase (as much of the Puna–Altiplano ignimbrites) that could cause magma chamber decompression. The resulting ignimbrites emplaced as poorly expanded dense flows that progressively evolved into viscous flows of similar behaviour to some large-volume silicic lava flows.

## Acknowledgements

I.A.P thanks funds from projects PICT 381, PIP 5255 and PIP 781. A. G is grateful for her Beatriu de Pinós post-doctoral fellowship 2008 BP B 0318. GAD acknowledges UNAM-PAPPIT grant IN-106109-3. We thank Michael Ort and Roberto Sulpizio for an earlier revision of this manuscript.

## References

Acocella, V., Cifelli, F., Funiciello, R., 2000. Analogue models of collapse calderas and resurgent domes. J. Volcanol. Geotherm. Res. 104, 81–96.

Acocella, V., Korme, T., Salvini, F., Funiciello, R., 2002. Elliptic calderas in the Ethiopian Rift: control of pre-existing structures. J. Volcanol. Geotherm. Res. 119, 189–203.

Acocella, V., Funiciello, R., Marotta, E., Orsi, G., de Vita, S., 2004. The role of extensional structures on experimental calderas and resurgence. J. Volcanol. Geotherm. Res. 129, 199–217.

Aguirre-Díaz, G.J., 2008. Types of collapse calderas: Collapse Calderas Workshop 19–25 October 2008, Querétaro, Mexico “Reconstructing the Evolution of Collapse Calderas: Magma Storage, Mobilization and Eruption”. IOP Conference Series: Earth and Environmental Science, 3 012021. doi:10.1088/1755-1307/3/1/012021 (5pp) http://www.iop.org/EJ/toc/1755-1315/3/1.

Aguirre-Díaz, G.J., Labarthe-Hernández, G., 2003. Fissure ignimbrites: fissure-source origin for voluminous ignimbrites of the Sierra Madre Occidental and its relationship with Basin and Range faulting. Geology 31, 773–776.

Aguirre-Díaz, G.J., Labarthe-Hernández, G., Tristán-González, M., Nieto-Obregón, J., Gutiérrez-Palomares, I., 2008. Ignimbrite Flare-up and graben-calderas of the Sierra Madre Occidental, Mexico. In: Gottsmann, J., Martí, J. (Eds.), Caldera volcanism: analysis, modelling and response. Developments in Volcanology, 10. Elsevier, Amsterdam. ISBN: 978-0-444-53165-0. 492 p., (143–180pp).

Argañaraz, R., Sureda, R., 1979. El yacimiento plumbífero “La Esperanza”, departamento La Poma, provincia de Salta, República Argentina. Asoc. Argent. Mineral., Petrología Sedimentol. 10 (3), 41-11.

Bellier, O., Sébrier, M., 1994. Relationship between tectonism and volcanism along the Great Sumatran Fault Zone deduced by SPOT image analyses. Tectonophysics 233, 215–231.

Blasco, G., Zappettini, E.O., Hongn, F., 1996. Hoja Geológica 2566-1, San Antonio de los Cobres. Programa Nacional de Cartas Geológicas de la República Argentina. Dir. Nac. del Servicio Geológico. Buenos Aires.

Carrapa, B., DeCelles, P., 2008. Eocene exhumation and basin development in the Puna of northwestern Argentina. Tectonics 27 (TC1015). doi:10.1029/2007TC002127.

Coira, B., Paris, G., 1981. Estratigrafía volcánica del área del cerro Tuzgle, Provincias de Jujuy y Salta. IIX Congreso Geológico Argentino III, pp. 659–671.

Coira, B., 1973. Resultados preliminares sobre la petrología del ciclo eruptivo Ordovícico concomitante con la sedimentación de la Formación Acoite en la zona de Abra Pampa, prov. de Jujuy. Asoc. Geol. Argent. Rev. 28, 85–88.

Coira, B., Kay, S.M., Viramonte, J., 1993. Upper Cenozoic magmatic evolution of the argentine Puna—a model for changing subduction geometry. Int. Geol. Rev. 35 (8), 677–720.

de Silva, S., Zandt, G., Trumbull, R., Viramonte, J.G., Salas, G., Jiménez, N., 2006. Large ignimbrite eruptions and volcano-tectonic depressions in the Central Andes: a thermomechanical perspective. In: Troise, C., De Natale, G., Kilburn, C.R. (Eds.), Mechanism of Activity and Unrest at Large Calderas, 269. Geological Society Special Publications, London, pp. 47–63.

Druitt, T.H., Sparks, R.S.J., 1982. A proximal ignimbrite breccia facies on Santorini volcano. Greece J. Volcanol. Geotherm. Res. 13, 147–171.

Francis, P.W., O'Callaghan, L., Kretzschmar, G.A., Thorpe, R.S., Sparks, R.S.J., Page, R.N., de Barrio, R.E., Gillio, G., Gonzalez, O.E., 1983. The Cerro Galan ignimbrite. Nature 301, 51–53. doi:10.1038/301051a0.

Geyer, A., Folch, A., Martí, J., 2006. Relationship between caldera collapse and magma chamber withdrawal: an experimental approach. J. Volcanol. Geotherm. Res. 157 (4), 375–386.

Gottsmann, J., Lavallée, Y., Martí, J., Aguirre-Díaz, G., 2009. Magma-tectonic interaction and the eruption of silicic batholiths. Earth Planet. Sci. Lett. 284, 426–434.

Guillou-Frottier, L., Burov, E.B., Milési, J.P., 2000. Genetic links between ash-flow calderas and associated ore deposits as revealed by large-scale thermo-mechanical modelling. J. Volcanol. Geotherm. Res. 102, 339–361.

Guzmán, S., Petrinovic, I., 2008. Pucarilla-Cerro Tipillas Volcanic Complex: the oldest recognized caldera in the southeastern portion of Central Volcanic Zone of Central Andes? Collapse Calderas Workshop IOP Conf. Series: Earth and Environmental Science, 3 012003. IOP Publishing. doi:10.1088/1755-1307/3/1/012003.

Guzmán, S., Petrinovic, I.A., Brod, J.A., 2006. Pleistocene mafic volcanoes and their relation with the boundary between the Puna and the Cordillera Oriental, Salta, Argentina. J. Volcanol. Geotherm. Res. 158 (1–2), 51–69.

Holohan, E.P., Troll, V.R., Walter, T.R., Münn, S., McDonnell, S., Shipton, Z.K., 2005. Elliptical calderas in active tectonic settings: an experimental approach. J. Volcanol. Geotherm. Res. 144, 119–136.

Holohan, E.P., van Wyk de Vries, B., Troll, V.R., 2008. Analogue models of caldera collapse in strike–slip tectonic regimes. Bull. Volcanol. 70, 773–796.

Hongn, F., del Papa, C., Powel, J., Petrinovic, I.A., Mon, R., Veraco, V., 2007. Middle Eocene deformation and sedimentation in the Puna–Eastern Cordillera transition (23°–26°S): inheritance of preexisting anisotropies on the pattern of initial Andean shortening. Geology 35 (3), 271–274.

Isacks, B., 1988. Uplift of the Central Andean Plateau and bending of the Bolivian orocline. J. Geophys. Res. 93, 3211–3231.

JICA, 1993. Informe sobre Exploración de Minerales del área Oeste de la República Argentina. Fase I (Marzo 1993) nº 17. Metal Mining Agency of Japan, unpublished.

López-Hernández, A., García-Estrada, G., Aguirre-Díaz, G., González-Partida, E., Palma-Guzmán, H., Quijano-León, J.L., 2009. Hydrothermal activity in the Tulancingo–Acoculco Caldera Complex, central Mexico: exploratory studies. Geothermics 38, 279–293. doi:10.1016/j.geothermics.2009.05.001.

Marret, R.A., Allmendiger, R.W., Alonso, R.N., Drake, R.E., 1994. Late Cenozoic tectonic evolution of the Puna plateau and adjacent foreland, norwestern Argentine Andes. J. S. Am. Earth Sci. 7, 179–208.

Marti, J., Ablay, G.J., Redshaw, L.T., Sparks, R.S.J., 1994. Experimental studies of collapse calderas. J. Geol. Soc. London 151, 919–929.

Martí, J., Geyer, A., Folch, A., 2009. A genetic classification of collapse calderas based on field studies, analogue and theoretical modeling. In: Thordarson, T., Self, S. (Eds.), Volcanology: the Legacy of GPL Walker. IAVCEI-Geological Society of London, London, pp. 249–266.

Martínez Reyes, J., Gonzalez Partida, E., Perez, R.J., Tinoco, M.J., 2008. Thermodynamic state updated of the volcanic caldera and geothermal reservoir of Los Humeros, Puebla, Mexico. Collapse Calderas Workshop IOP Publishing IOP Conf. Series: Earth and Environmental Science, 3, p. 012014. doi:10.1088/1755-1307/3/1/012014.

Matteini, M., Mazzuoli, R., Omarini, R., Cas, R., Maas, R., 2002. The geochemical variations of the upper Cenozoic volcanism along the Calama–Olacapato–El Toro transversal fault system in the central Andes (24°S): petrogenetic and geodynamic implications. Tectonophysics 345, 211–227.

Mazzuoli, R., Vezzoli, L., Omarini, R., Acocella, V., Gioncada, A., Matteini, M., Dini, A., Guillou, H., Hauser, N., Uttini, A., Scaillet, S., 2008. Miocene magmatism and tectonics of the easternmost sector of the Calama–Olacapato–El Toro fault system in Central Andes at 24°S: insights into the evolution of the Eastern Cordillera. GSA Bulletin 120 (11–12), 1493–1517. doi:10.1130/B26109.1.

Olson S.F. and Gilzean, N., 1987. Regional Geology of the Nevado Queva Area. BHP Minerals & Co, Argentina, Unpublished.

Petrinovic, I.A., 1994. Volcanismo Cenozoico asociado al lineamiento Calama–Olacapato–El Toro en el tramo comprendido entre San Antonio de los Cobres y Olacapato, provincia de Salta, Argentina. Phd Thesis Universidad Nacional de Salta, Argentina. 234 p. Unpublished.

Petrinovic, I.A., 1999. La Caldera de colapso del Cerro Aguas Calientes, Salta; República Argentina; Evolución y Esquema Estructural. In: Colombo, F., Queralt I. and Petrinovic, I.A. (Eds.) Geología de los Andes Centrales Meridionales: El Noroeste Argentino. Acta Geol. Hisp. 34, 243–255.

Petrinovic, I.A., Colombo, F., 2006. Phreatic to Phreatomagmatic eruptions in the Tocomar volcanic centre, Puna, Argentina. J. Volcanol. Geotherm. Res. 158 (1–2), 37–50.

Petrinovic, I.A., Mitjavila, J., Viramonte, J.G., Marti, J., Becchio, R., Arnosio, M., Colombo, F., 1999. Geoquímica y Geocronología de secuencias volcánicas Neógenas de trasarco, en el extremo oriental de la Cadena Volcánica Transversal del COT, noroeste de Argentina. In: Colombo, F., Queralt, I., Petrinovic, I.A. (Eds.), Geología de los Andes Centrales Meridionales: El Noroeste Argentino, Acta Geológica Hispánica, 34 (2–3), pp. 255–273.

Petrinovic, I.A., Riller, U., Brod, A., 2005. The Negra Muerta volcanic complex, southern Central Andes: geochemical characteristics and magmatic evolution of an episodic volcanic centre. J. Volcanol. Geotherm. Res. 140 (4), 295–320. doi:10.1016/j.jvolgeores.2004.09.002.

Petrinovic, I.A., Riller, U., Alvarado, G., Brod, J.A., Arnosio, M., 2006. Bimodal volcanism in a tectonic transfer zone: evidence for tectonically controlled magmatism in the southern Central Andes, NW Argentina. J. Volcanol. Geotherm. Res. 152, 240–252.

Petrinovic, Ivan A., Hongn, F.D., del Papa, C.E., Caffe, P.J., 2008. (Central Andes): tectonic and magmatic implications by Acocella, et al. [Tectonophysics 434 (2007) 81–92]. Tectonophysics 469 (1–4), 150–154.

Ramelow, J., Riller, U., Romer, R., Onceen, O., 2005. Kinematic link between episodic trapdoor collapse of the Negra Muerta Caldera and motion on the Olacapato–El Toro Fault Zone, southern central. Int. J. Earth Sci. (Geol. Rundsch.). doi:10.1007/s00531-005-0042-x.

Riller, U., Oncken, O., 2003. Growth of the central Andean Plateau by tectonic segmentation is controlled by the gradient in crustal shortening. J. Geol. 111, 367–384.

Riller, U., Petrinovic, I., Ramelow, J., Greskowiak, J., Strecker, M., Oncken, O., 2001. Late Cenozoic tectonism, caldera and plateau formation in the central Andes. Earth Planet. Sci. Lett. 188, 299–311.

Saint Blanquat, M., Tikoff, B., Teyssier, C., Vigeresse, L.J., 1998. Transpressional kinematics and magmatic arcs. In: Holdsworth, R.E., Strachan, R.A., Dewey, J.F. (Eds.), Continental Transpressional Tectonics: Geological Society, London, Special Publications, 135, pp. 327–340.

Salfity, J.A., 1985. Lineamientos Transversales al rumbo andino en el noroeste argentino. IV Congreso Geológico de Chile, Antofagasta II, pp. 119–137.

Soler, M., Caffe, P., Coira, B., Kay, S.M., Takashi, O.A., 2007. Geology of the Vilama caldera: a new interpretation of a large scale explosive event in the Central Andean plateau during the Upper Miocene. J. Volcanol. Geotherm. Res. 164 (1–2), 27–53.

Soriano, C., Zafrilla, S., Martí, J., Ablay, G.J., Cas, R.A.F., Bryan, S., 2002. Welding and rheomorphism of phonolitic fallout deposits from the Las Cañadas caldera (Tenerife, Canary Islands). Geol. Soc. Am. Bull. 114 (7), 883–895.

Spinks, K.D., Acocella, V., Cole, J.W., Bassett, K.N., 2005. Structural control of volcanism and caldera development in the transitional Taupo volcanic Zone, New Zealand. J. Volcanol. Geotherm. Res. 144, 7–22.

Suárez, M., Márquez, M., 2007. A Toarcian retro-arc basin of Central Patagonia (Chubut), Argentina: Middle Jurassic closure arc migration and tectonic setting. Rev. Geol. Chile 34 (1), 63–79.

Sureda, R.J., Galliski, M.A., Argañaraz, P., Daroca, J., 1986. Aspectos metalogénicos del Noroeste argentino (provincias de Salta y Jujuy). Capricornio I, 39–95.

Turner, J.C.M., 1964. Descripción de la Hoja Geológica 7c, Nevado de Cachi, Salta: Dirección Nacional de Geología y Minería, Boletín N 99. .

Vigneresse, J.L., 2007. The role of discontinuous magma inputs in felsic magma and ore generation. Ore Geol. Rev. 30, 181–216.

Viramonte, J.G., Petrinovic, I.A., 1990. Cryptic and partially buried calderas over a strike–slip fault system in the Central Andes. 2nd International Symposium on Andean Geodynamics, Grenoble, pp. 313–315.

Viramonte, J.M., Becchio, R., Viramonte, J., Pimentel, M., Martino, R., 2007. Ordovician Igneous and metamorphic units in the southern Puna: new U/Pb and Sm/Nd data and implications for the evolution of NW Argentina. J. South Am. Earth Sci. 24 (2–4), 167–183.